Jinst

Published by IOP Publishing for Sissa Medialab

Received: *September 30, 2019*
Accepted: *January 21, 2020*
Published: *February 18, 2020*

21st International Workshop on Radiation Imaging Detectors
7–12 July 2019
Crete, Greece

First full dynamic range scan of the JUNGFRAU detector performed at an XFEL with an accurate intensity reference

S. Redford,[a,1] **M. Andrä,**[a] **R. Barten,**[a] **A. Bergamaschi,**[a] **M. Brückner,**[a] **S. Chiriotti,**[a] **R. Dinapoli,**[a] **E. Fröjdh,**[a] **D. Greiffenberg,**[a] **K.S. Kim,**[b] **J.H. Lee,**[b] **C. Lopez-Cuenca,**[a] **M. Meyer,**[a] **D. Mezza,**[a] **A. Mozzanica,**[a] **S.-Y. Park,**[b] **C. Ruder,**[a] **B. Schmitt,**[a] **X. Shi,**[a] **D. Thattil,**[a] **G. Tinti,**[a] **S. Vetter**[a] **and J. Zhang**[a]

[a] *Paul Scherrer Institut,*
Villigen 5232, Switzerland
[b] *Pohang Accelerator Laboratory,*
Pohang, Gyeongbuk 37673, Republic of Korea

E-mail: sophie.redford@psi.ch

Abstract: JUNGFRAU is a charge integrating hybrid silicon pixel detector primarily designed to equip SwissFEL, the free electron laser at the Paul Scherrer Institut. The charge integrating architecture ensures responsiveness to the brilliant, short (~ 10 fs) pulses of photons, while three dynamically switching gains ensure single photon sensitivity above 2 keV and a high dynamic range of 10^4 12 keV photons. These proceedings detail the first full dynamic range scan of the JUNGFRAU performed at an XFEL in controlled conditions. A robust and accurate intensity measurement is achieved by counting the number of photons detected in an attenuated area of the detector. The scan provides a fascinating study into the response as a function of intensity, and allows the accuracy of the standard correction procedure to be quantified. The calibration constants, routinely calculated at PSI, and the pedestal offsets, typically measured by forced switching in dark conditions, are shown to be good. Small differences between results from the two methods lead to ideas and proposals for future measurements.

Keywords: Instrumentation for FEL; Instrumentation for synchrotron radiation accelerators; X-ray detectors

[1] Corresponding author.

https://doi.org/10.1088/1748-0221/15/02/C02025

Contents

2020 JINST 15 C02025

1 Introduction

JUNGFRAU is a hybrid silicon pixel detector designed and developed at PSI to equip beamlines of X-ray Free Electron Lasers (XFELs) in particular SwissFEL [1]. Three automatically switching gain stages ensure both single photon sensitivity and a dynamic range of 10^4 12 keV photons [2]. As a charge integrating detector, JUNGFRAU can record the extremely fast (fs duration) pulses of photons which impinge on the sensor. However, the raw output of the JUNGFRAU must be corrected per pixel for pedestal levels and gains before the deposited energy or the number of photons detected is retrieved. It is therefore of paramount importance that pedestals and gains of each pixel are well known.

The standard way to obtain the correction values occurs in two steps. First, during the construction of the system, a calibration procedure is performed at PSI to determine the gain constants of each pixel [3]. This uses three different, overlapping sources of charge to cover the dynamic range. Second, pedestals are measured by forcing the gain switching during dark conditions [4]. This must be done in the same conditions as the experiment itself and hence can't be prepared in advance.

These proceedings present an intensity scan which was recorded at the PAL-XFEL in March 2019. For the first time, the full dynamic range of the JUNGFRAU was probed at an XFEL, with an accurate intensity measurement. This data allows the standard correction procedure to be tested in more detail than was possible before. Section 2 details the experimental setup, and section 3 discusses the typical JUNGFRAU response to the intensity scan. Section 4 shows an improved intensity measurement. Sections 5 and 6 present data corrected by the parameters extracted from the intensity scan itself and the standard method respectively. Section 7 compares the closed-loop derived corrections to the standard ones. Section 8 summarises and discusses future steps.

2 Experimental setup

The four Mpixel JUNGFRAU detector installed at the XSS beamline of the PAL-XFEL [5] was used, see figure 1a. This system was designed in-house with a central beam pipe and four quadrants of detector modules, each rotated 90° with respect to the neighbour. It is equipped with eight calibrated JUNGFRAU modules and eight standard readout boards provided by PSI.

The XFEL operated at 12.705 keV without monochromator, to increase the spread of energies. To cover the full dynamic range of the detector, seventeen different combinations of attenuators were used, providing transmissions from 10^{-4} to 1. This measurement benefits from the natural shot-to-shot fluctuations of the XFEL. Four photo-diodes are positioned symmetrically around a scatter foil in the beam before the attenuators. The sum of the four photo-diode readings per shot multiplied by the transmission factor gives a measurement proportional to the intensity of the beam. The XFEL beam hit a Copper target, which was angled to ensure a grazing incidence. The resultant Copper fluorescence photons impinged on the lower right hand quadrant of the detector, which was mounted at 90° to the beam and 5 cm from the Copper target. The top right hand quadrant of the detector was covered with 500 µm of Aluminium foil, to reduce the flux in this area and aid with the intensity measurement (see section 4). A typical image recorded during the measurement is shown in figure 1b. One thousand images were recorded per attenuation step.

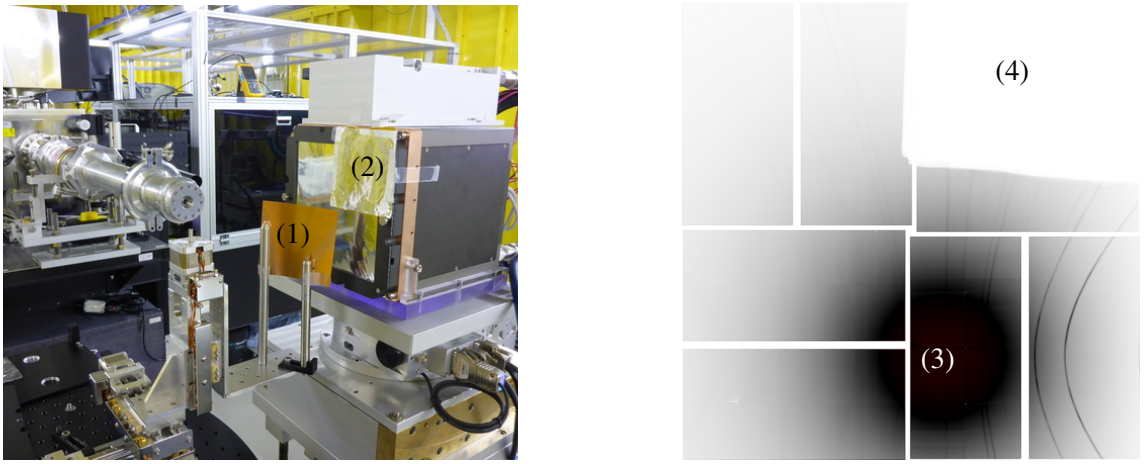

(a) **(b)**

Figure 1. (a) Photograph of the experimental setup. The silver-coloured beampipe is visible on the left. The beam grazes on the Copper target (1), and fluorescent photons impinge onto the four Mpixel JUNGFRAU detector. One quadrant of the detector is covered with 500 um Aluminium foil (2). (b) Typical image recorded during the scan, looking from the incoming photon direction. The highest intensity is in the lower right quadrant (3). The upper right quadrant is shielded by the foil (4).

3 JUNGFRAU response to the intensity scan

The response of one pixel of the detector during the intensity scan is shown in figure 2a. On the x-axis is the intensity, calculated by multiplying the relevant dimensionless transmission coefficient (att. transmission) by the photo-diode measured shot intensity (Diode I_0) in units of Coulombs. On

2020 JINST 15 C02025

the y-axis is the JUNGFRAU (JF) response in ADU units. The three gains of the JUNGFRAU are evident, high (blue), medium (green) and low (red). The change in slope sign from high to medium gain is due to the removal of the CDS [2]. The entire dynamic range of this pixel was probed, from pedestal in high gain to saturation in low gain.

The response as a function of intensity is fit with a linear function, per pixel and per gain, to give information on the linearity, the ratio of the gains (to compare with calibration measurements) and the intercepts (to compare with forced gain switching pedestals). The intensity range over which the data is fit needs careful consideration. Regarding the two gain switching areas: Poisson fluctuations in the number of photons striking the target pixel mean that shots with the same nominal intensity can be recorded in a higher or lower gain. This leads to an apparent non-linearity in the gain switching areas. To avoid this bias, the intensity region in which two gains are present is ignored, see figure 2b. Regarding the saturation area: shots above saturation cause a plateau in the JUNGFRAU response leading to an apparent non-linearity. To avoid this bias, the higher limit of low gain is the first point at which saturation occurs.

With these considerations in mind, the response shown in figure 2a was fit with three linear functions. Figure 2c shows the residuals to the fit in low gain. It is clear that the seventeen attenuation coefficients are not quite correct, whereas the photo-diode measurements within each attenuation step do show a response proportional to that of the JUNGFRAU.

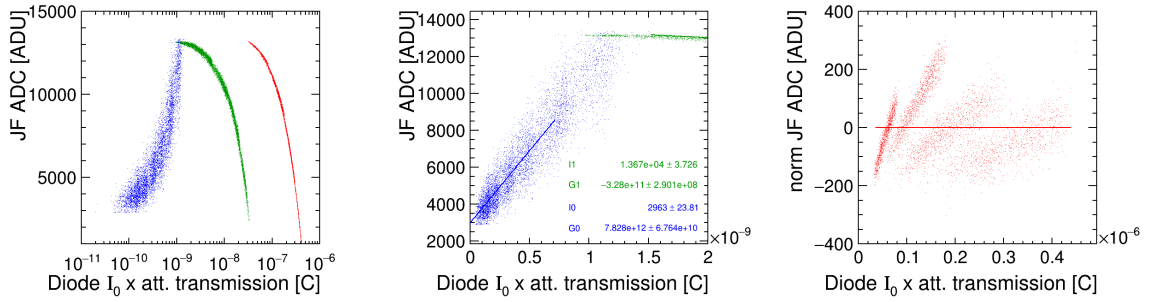

Figure 2. (a) Response of a typical JUNGFRAU pixel to the intensity scan, as a function of the photo-diode measured shot intensity multiplied by the transmission factor of the beamline attenuators. (b) Fit in high and medium gains. The data points around intensity of 1×10^{-9} are not fit, to avoid the bias introduced by gain switching. (c) Residual of fit in low gain, showing discontinuities caused by incorrect attenuation factors.

4 Improved intensity estimate by counting photons behind the foil

An improved intensity estimate was devised by counting the number of photons detected behind the attenuating foil in each frame. This should be, within Poisson statistics, proportional to the shot intensity. A pixel mask was determined to avoid bad pixels from contributing to the count. The mask includes: pixels not in high gain during dark conditions; pixels with pedestal RMS higher than 30 ADU; pixels which switch to medium gain in the intensity scan; pixels in several predefined rectangular areas, where more intense spots, rather than isolated photons, fell on the detector; multi-size pixels; unresponsive pixels; pixels with failed fits to the noise and first photon peak.

2020 JINST 15 C02025

Unexpectedly, photons behind the foil have beam energy, see figure 3, and must be scattered somewhere upstream. Nevertheless, the number of photons should still scale with shot intensity. Third harmonics of the beam are present, so it was not possible to count the photons by rounding the pedestal and gain corrected ADC values to integer. Instead, at low intensity the number of photons in the zero and first photon peaks were used to estimate the Poisson mean and then, multiplying by the number of active pixels, the total number of photons. At the chosen transition intensity of 4×10^4 counted photons, the difference between the scaled Poisson mean and the number of rounded photons (2%) is used to correct the number of rounded photons, and this scaled number of photons is used for the rest of the range, creating the 'Nphotons behind foil' variable.

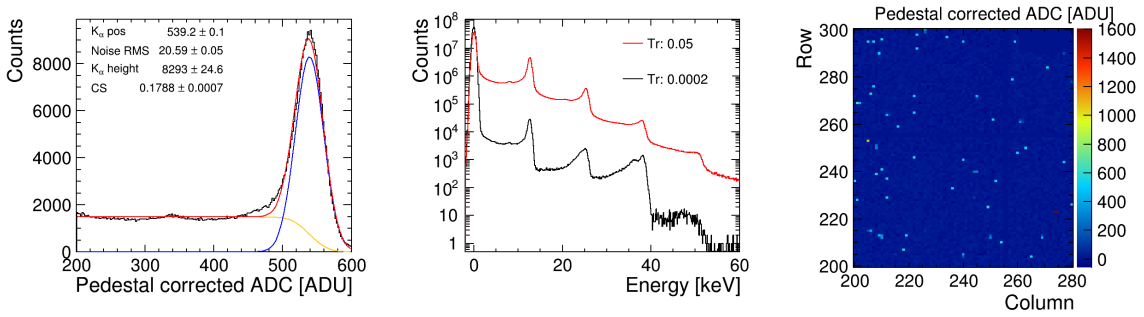

Figure 3. (a) Fit to the first photon peak to give the gain in ADU. The small peak at 320 ADU is from Copper fluorescence photons. (b) Energy spectra behind the foil, showing the presence of 3rd harmonics in the low transmission data. (c) Pedestal corrected image showing photons behind the foil at 0.2% transmission.

The number of counted photons behind the foil correlates well with the photo-diode measured intensity in each transmission step, see figure 4a. Fitting the response as a function of number of photons counted behind the foil (figure 4b) results in residuals without discontinuity or non-linearity, see figure 4c. Counting the photons behind the foil provides a more robust and accurate intensity measurement than the transmission factors multiplied by the photo-diode measurements.

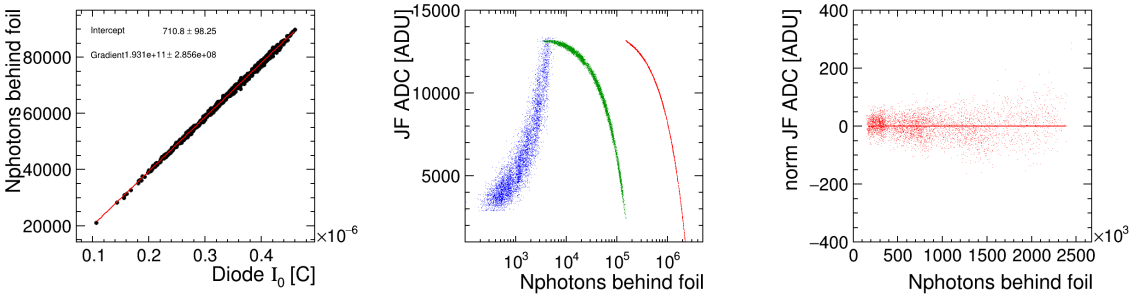

Figure 4. (a) Correlation between number of photons counted behind the foil and photo-diode measured intensity at 4% transmission. (b) Response of a typical JUNGFRAU pixel to the intensity scan, as a function of the number of photons counted behind the foil. (c) Residual of fit in low gain, showing no discontinuity or non-linearity. (b) and (c) can be compared to the plots in figure 2, since the same pixel is plotted.

2020 JINST 15 C02025

5 Determining and applying closed-loop corrections to the scan data

Without using any additional calibration or pedestal datasets, the intensity scan data can be used to correct itself in a 'closed-loop' fashion. The algorithm is the following: on a per-pixel basis, the noise and first photon peak are fitted to give an absolute calibration of high gain, see figures 5a and 5b. This calibration is extended to medium and low gains by fitting the response curves of the three gains with linear functions between the ranges described in section 3 and measuring the per-pixel ratio of fitted gradients, see figure 5c. This mimics the standard calibration procedure detailed in [3]. The fit intercepts, per pixel and per gain, are taken as the pedestals.

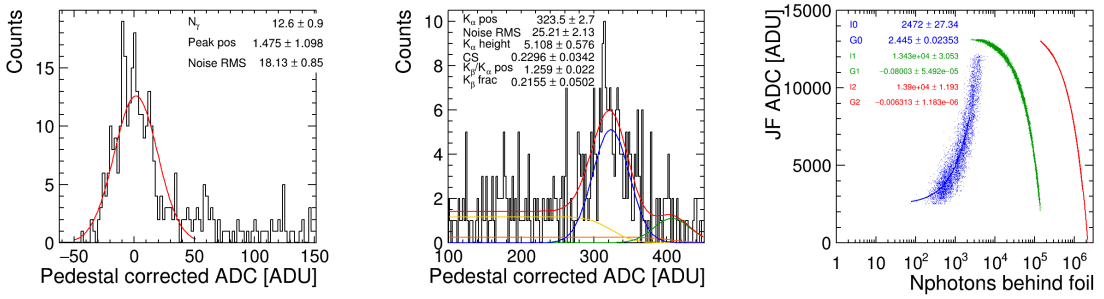

(a) **(b)** **(c)**

Figure 5. Determination of pedestal and gain corrections from the intensity scan. (a) Gaussian fit to the noise peak of a single pixel in pedestal corrected data. (b) Fit to the Copper fluorescence K_α and K_β peaks of a single pixel in pedestal corrected data. (c) Linear fit of the three gains for a typical pixel.

Closed-loop corrected data of one pixel can be seen in figure 6. The three gains are fit between the same ranges as determined in section 3. By definition, the fit intercepts of all three gains are zero within uncertainties, and the fit gradients of medium and low gain match that of high gain. Of particular interest in this test are the gain switching points (figures 6b and 6c), which should show continuous, overlapping data, as is the case for the pixel shown here.

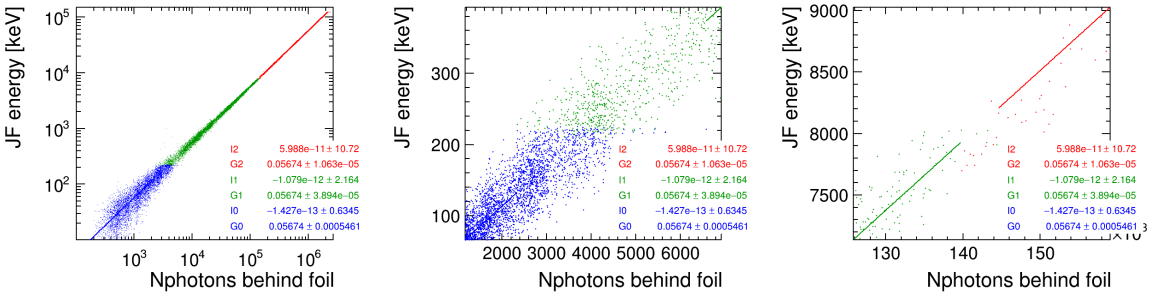

(a) **(b)** **(c)**

Figure 6. Self correction of one pixel of the intensity scan, with ADC converted to energy. (a) Full dynamic range. (b) High to medium gain switching range. (c) Medium to low gain switching range.

The overlap was measured per pixel for both gain switching regions, by subtracting the lowest energy measured in the lower gain from the highest energy measured in the higher gain. This

2020 JINST 15 C02025

should always result in a negative (an overlap). While the transition from medium to low gain overlaps in 98% of pixels, 48% of pixels exhibit a 'gap' between high and medium gains. Figure 7a shows this for an affected pixel. This pixel will never return an energy of 280 keV. Considering the overlap across many pixels, some structure is present, see figure 7b. For the module shown here, the eight chips (in 4×2 arrangement) are visible, as are the four vertical 'supercolumns' per chip corresponding to the multiplexers and off-chip drivers. Given that the effect is worst in the chips with highest intensity, we wonder if this is a powering issue which comes to light when many pixels in the same chip switch together.

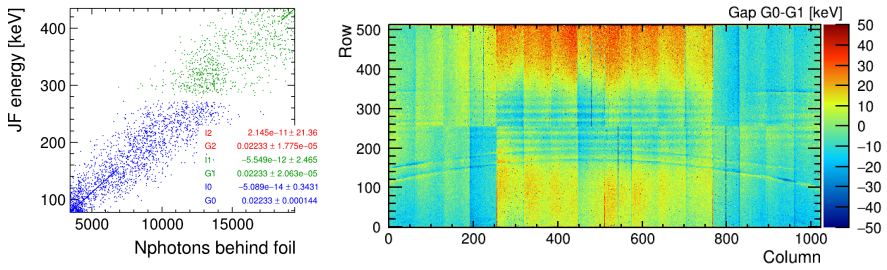

(a) **(b)**

Figure 7. (a) Self-corrected data for a single pixel, showing a gap between high and medium gain at around 280 keV. (b) High to medium gain gap size as a function of pixel position on the module. Positive denotes a gap (unexpected response). While some intensity of illumination features are visible as ripples, the effect is worst for the outer edges of the central chips.

6 Applying standard corrections to the scan data

The intensity scan dataset was also corrected in the standard manner, using forced gain switching pedestals and the calibration constants measured previously at PSI, see figure 8. Figures 6 and 8 can be directly compared since the same pixel is shown. The results are broadly as expected, showing that the standard correction procedure is working well.

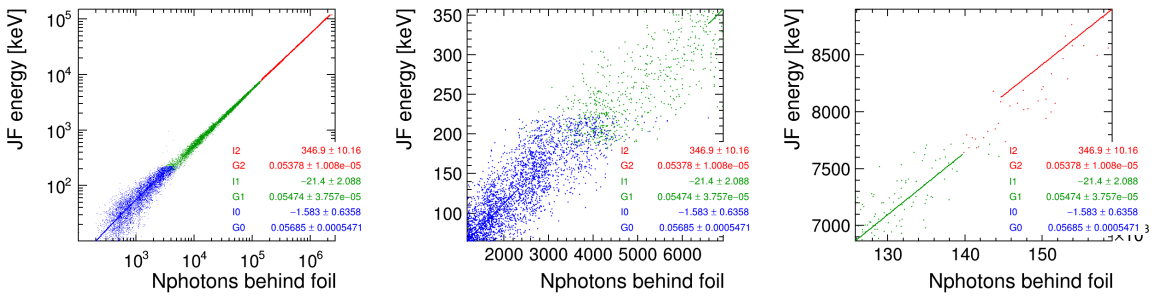

(a) **(b)** **(c)**

Figure 8. Standard correction of one pixel of the intensity scan. (a) Full dynamic range. (b) High to medium gain switching range. (c) Medium to low gain switching range.

2020 JINST 15 C02025

7 Comparing standard and closed-loop corrections

High gain factors derived at PSI and PAL agree well. The distribution of the pixel-wise percentage difference is Gaussian with $\mu = (0.2123 \pm 0.0029)\%$ and $\sigma = (2.047 \pm 0.003)\%$. The uncertainty on the PAL-measured factors is significant (1%) due to the low statistics in the single photon regime. The level of agreement is therefore satisfactory. The pull distribution has a width of 1.2σ.

Concerning medium and low gain factors, ratios derived at PSI and PAL agree to within a few percent, see figure 9. Some dependence following the illumination is visible, in particular the high intensity rings which moved slightly on the detector during the scan. The average PSI-PAL difference is 3% for high/medium gain, and 2% for medium/low gain.

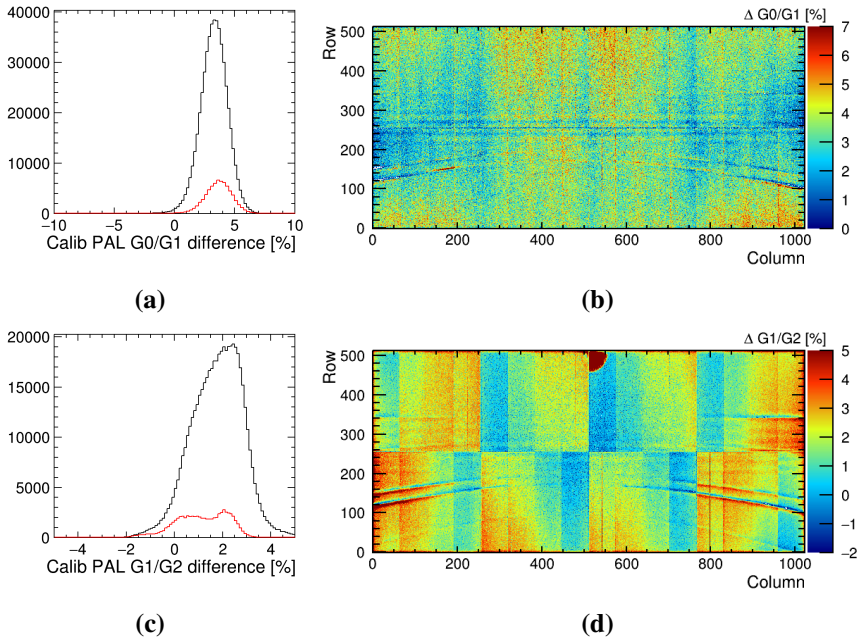

Figure 9. Percent difference between PSI and PAL high/medium (a,b) and medium/low (c,d) ratios. The red line shows only pixels which reached saturation.

The high gain pedestals are on average 40 ADU higher than the high gain intercepts. This offset is caused by the small non-linearity in the pixel buffer [3]. Figure 3b of [3] demonstrates that fitting the whole high gain range will result in an offset between intercept and pedestal of (in the case of the target pixel there) 32 ADU, which is consistent with the distribution of offsets presented here. Restricting the high gain fit range of the intensity scan to only the pedestal and the first two photon peaks, the high gain pedestals and intercepts are consistent, although now with much higher uncertainty in the intercept due to the low statistics.

The forced gain switching pedestals were compared to the intercept points of medium and low gain, see figure 10. The forced switching for medium gain measures around 30 ADU lower than the intercept. The forced switching for low gain measures on average 40 ADU higher than the intercept. This is unexpected. Since medium and low gain both have a negative response gradient, it was expected that any pedestal-intercept differences would also be in the same direction. More measurements will be necessary to understand the effect.

2020 JINST 15 C02025

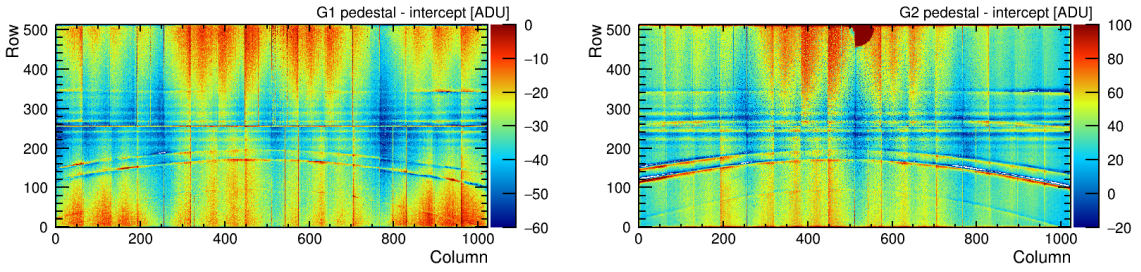

(a) **(b)**

Figure 10. Difference between medium (a) and low (b) gain forced gain switching pedestals and fit intercepts.

8 Summary

For the first time, the full dynamic range of the JUNGFRAU was scanned at an XFEL with an accompanying accurate shot intensity measurement. The linear response of the charge integrating JUNGFRAU detector to the fs duration FEL pulses was demonstrated over four orders of magnitude. The standard correction procedure, using forced gain switching pedestals and calibration constants measured at PSI, was validated and shown to work sufficiently well. Detailed comparison between standard and closed-loop corrections reveal differences of the order of a few %.

There are several possibilities to build on and extend the research presented here. When such an intensity scan can be repeated, it would be interesting to use a shield to restrict the illuminated area of the detector. This would eliminate effects originating from multiple pixels switching gain simultaneously. A new ASIC JUNGFRAU1.1 under test at the time of writing also brings opportunities. The current source should extend down into high gain, allowing a more robust measurement of the high to medium gain ratio. Forced gain switching will be possible on a column-wise basis, allowing pedestals to be recorded in less power-stressful situations.

Acknowledgments

The experiments were performed at beamline XSS of PAL-XFEL funded by the Ministry of Science and ICT of Korea. We thank the beamline staff and detector group, in particular Seungyu Rah, Seonghan Kim and Hyojung Hyun for their support, collaboration and the use of their JF4M.

References

[1] C. Milne, T. Schietinger, M. Aiba, A. Alarcon, J. Alex, A. Anghel et al., *SwissFEL: The Swiss X-ray Free Electron Laser*, *Appl. Sci.* **7** (2017) 720.

[2] A. Mozzanica et al., *Characterization results of the JUNGFRAU full scale readout ASIC*, 2016 *JINST* **11** C02047.

[3] S. Redford et al., *First full dynamic range calibration of the JUNGFRAU photon detector*, 2018 *JINST* **13** C01027.

[4] S. Redford et al., *Operation and performance of the JUNGFRAU photon detector during first FEL and synchrotron experiments*, 2018 *JINST* **13** C11006.

[5] H.-S. Kang, C.-K. Min, H. Heo, C. Kim, H. Yang, G. Kim et al., *Hard X-ray free-electron laser with femtosecond-scale timing jitter*, *Nat. Phot.* **11** (2017) 708.